Contact Angle Saturation in Electrowetting

Anthony Quinn, Rossen Sedev, and John Ralston*

Ian Wark Research Institute, University of South Australia, Mawson Lakes, Adelaide, South Australia 5095, Australia

Received: July 7, 2004

Electrowetting is the phenomenon of contact angle decrease under the influence of an external voltage applied across the solid/liquid interface. Electrowetting offers an interesting possibility to enhance the wettability of hydrophobic materials without altering the chemical composition of the system and thus could be incorporated in various microfluidic devices. Electrowetting is fundamentally an electrocapillary effect occurring on an insulated solid electrode (hence the change of the solid/liquid interfacial tension with voltage follows Lippmann's equation). A limiting contact angle value larger than zero is achieved even at very large external voltages. Saturation precludes full wetting of the substrate and restricts the magnitude of the capillary force variation. Contact angle saturation has been given various interpretations (e.g., charge trapping, air ionization) but appears to reflect a natural thermodynamic limit rather than being simply a defective property. The limiting value of the contact angle is given by the Young equation when the value of the solid/liquid interfacial tension reaches zero. The model is in excellent agreement with our own results and often gives an adequate description of published data. It also suggests that the saturation limit is determined by the material properties of the system and electrowetting at voltages exceeding this threshold is essentially a nonequilibrium process.

Introduction

The wettability of solid materials is of paramount importance in many natural and industrial processes. Most often the wetting properties of a given system are modified by altering the system, for example, pretreatment of the solid surface, introduction of additives into the liquid, etc. The application of an external voltage has long been known to affect the contact angle and has recently resurfaced as an attractive way to manipulate wettability without changing the chemical composition of the contacting phases.[1−14]

Electrowetting is the phenomenon of enhancing the wettability of a solid material with respect to a given liquid by applying an external voltage across the solid/liquid interface.[15] The most popular experimental configuration is sketched in Figure 1.

A drop of aqueous electrolyte solution is placed on top of an insulated electrode (Au) and is contacted by a platinum electrode. When voltage is applied, the liquid drop spreads further, i.e., the contact angle decreases. We have recently reiterated that electrowetting is essentially an electrocapillary phenomenon taking place on a solid interface as well as canvassing some of the historical developments of the subject.[14]

The initial contact angle, i.e., the one measured without any external voltage, can be dramatically altered (often by 50% or more), and therefore electrowetting offers an excellent option for moving (small) amounts of liquid over a hydrophobic surface. Indeed several ingenious prototypes have been constructed such as liquid micromanipulation,[16−19] liquid movement in capillary arrays,[20] a liquid lens with variable focal length,[21] tuning of the focal length of liquid lenses before photopolymerization,[22] and electronic paper.[23] The potential applications are of significant interest, and unsurprisingly, the number of publications on the topic has doubled over the last couple of years.

* Author to whom correspondence should be addressed. E-mail: john.ralston@unisa.edu.au

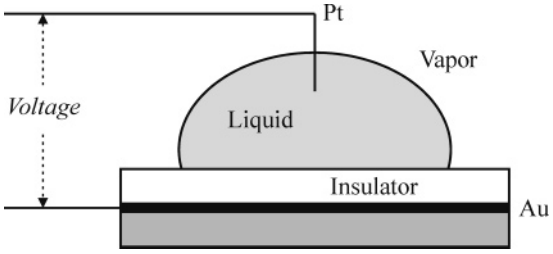

Figure 1. Electrowetting experiment. Voltage (dc or ac) from an external source is applied across the solid/liquid interface. The Au electrode is covered with a thin polymer layer, which is insulating and also hydrophobic; the upper electrode is a thin Pt wire; the droplet is an electrolyte solution and is conductive.

One major objective in electrowetting studies is to maximize the accessible contact angle range ("electrowetting modulation" in the engineering vernacular). The main obstacle is the fact that (after some initial contact angle decrease) even very large external voltages fail to achieve full wetting, i.e., zero contact angle. It is often perceived that this saturation phenomenon is a device-related imperfection that could be remedied through better engineering. Interestingly, the basic physics of the phenomenon has not been fully clarified. Several rather disconnected hypotheses have been advanced such as charge trapping,[12] gas ionization in the vicinity of the contact line,[11] contact line instability,[11] droplet resistance,[24] and the zero interfacial tension criterion.[13]

In this paper, we expand the hypothesis of zero solid/liquid interfacial tension and present an extensive evaluation of available experimental data as well as an examination of the kinetic behavior and the difference between alternating current (ac) and direct current (dc) voltages. The overall conclusion is that our simple saturation model is quite reliable in predicting the limit of validity of the Young−Lippmann equation.

10.1021/jp040478f CCC: $30.25
Published on Web 03/11/2005

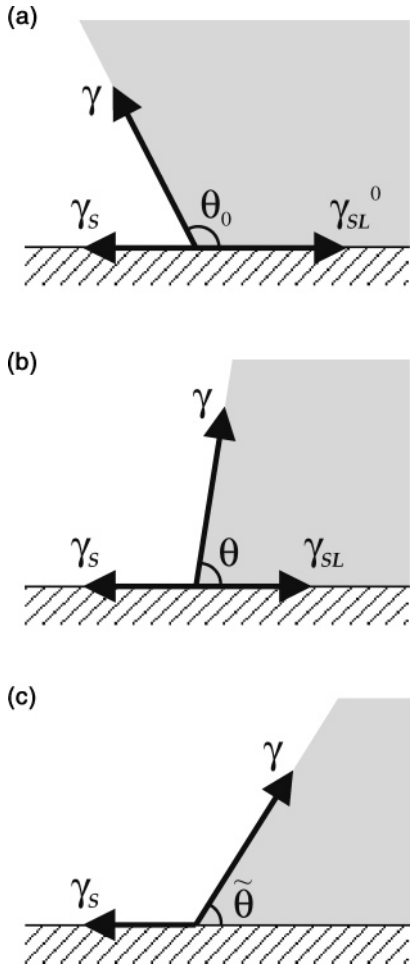

Figure 2. Saturation model. (a) No external voltage; the contact angle θ_0 is related to γ_S, γ, and γ_{SL}^0 via Young eq 1; (b) when external voltage is applied, γ_{SL} effectively decreases (eq 5) and so does the contact angle $\theta < \theta_0$ (Young−Lippmann eq 8); (c) at saturation, $\gamma_{SL} = 0$, and the contact angle has reached its limiting value $\tilde{\theta}$ (eq 3).

Saturation Model

Our analysis is based on the Young equation, which is the equilibrium condition for a three-phase contact line.[25−27] It predicts a unique contact angle, θ, for any given three-phase system (Figure 2a)

$$\gamma_S - \gamma_{SL} = \gamma \cos\theta \tag{1}$$

where γ_S, γ_{SL}, and γ are the interfacial tensions of the solid/gas, solid/liquid, and liquid/gas interfaces.

We ignore any complications related to contact angle hysteresis. This simplification appears plausible since the hysteresis we typically observe on a carefully prepared fluoropolymer surface is less than 10°.[8,14] The equilibrium condition eq 1 also applies at any external voltage, V, and thus we have (Figure 2b)

$$\cos\theta(V) = \frac{\gamma_S - \gamma_{SL}(V)}{\gamma} \tag{2}$$

The contact angle dependence on the external voltage is entirely ascribed to changes in the solid/liquid interfacial tension, γ_{SL}, while both γ and γ_S are assumed to be potential independent. There are reports that the interfacial tension of a pure liquid may be slightly influenced by the application of an electric field, but the voltage required is much larger (~4000 V and above[28−30]) than the highest voltages typically applied in electrowetting experiments (~100−200 V). As for the solid/gas interface, we follow Frumkin's reasoning[31,32] that γ_S should not be altered in the configuration depicted in Figure 1.

It is widely recognized that the terms entering the Young eq 1 are interfacial tensions[27,33−37] and since tension cannot be negative its lowest possible value is zero. Thus, the limiting value of the contact angle, $\tilde{\theta}$, under electrowetting conditions must be[13] (Figure 2c)

$$\cos\tilde{\theta} = \frac{\gamma_S}{\gamma} \tag{3}$$

According to eq 3, the saturation contact angle is completely determined by the material properties of the system (incorporated in γ_S and γ). In all cases of interest, the contact angle without external voltage is greater than zero, which implies that the liquid surface tension is higher than the surface tension of the solid.[25] In other words, we do not expect the limiting angle $\tilde{\theta}$ to be zero (contrary to the intuitive perception[38]). Thus, within our model, electrowetting saturation is not a defective phenomenon[6] but rather the consequence of reaching a thermodynamic limit of stability.

We have reiterated previously[14] that electrowetting is an electrocapillary phenomenon happening at a solid/liquid interface. Consequently the change of the interfacial tension with potential is related to the surface charge density, σ, by the Lippmann equation[39]

$$\sigma = -\frac{\partial\gamma_{SL}}{\partial V} \tag{4}$$

where the derivative is taken at constant temperature, pressure, and chemical composition.

The capacitance of the system is mainly determined by the capacitance of the insulating layer[5,40,41] and is therefore constant. From eq 4, we obtain

$$\gamma_{SL}(V) = \gamma_{SL}^0 - \frac{1}{2}CV^2 \tag{5}$$

where γ_{SL}^0 is the interfacial tension at the point of zero charge, i.e., the chemical part of γ_{SL},[42,43] and C is the capacitance per unit area. The foundations of this equation and its relationship to the overall free energy minimization of the system are dealt with elegantly elsewhere[12,14,32,39,44]. The threshold voltage for saturation, $\tilde{V}$, is therefore

$$\tilde{V} = \left(\frac{2\gamma_{SL}^0}{C}\right)^{1/2} = \left[\frac{2(\gamma_S - \gamma\cos\theta_0)}{C}\right]^{1/2} \tag{6}$$

where the contact angle at zero external voltage, θ_0, was used to express γ_{SL}^0 (which is not directly measurable) through the Young eq 1. Finally, to make use of eq 6, we need an appropriate value of γ_S. It is widely agreed that a consistent γ_S value may be deduced from experimentally obtained contact angles and various (often divergent) theoretical paths have been proposed (e.g., refs 34 and 45 and references therein). Since the debate is not entirely over, we adopt the approximation that the surface tension of the solid γ_S is numerically identical to the critical surface tension of wetting, γ_C, as defined by Zisman.[25,46] For apolar surfaces (like Teflon AF), this is a well-founded

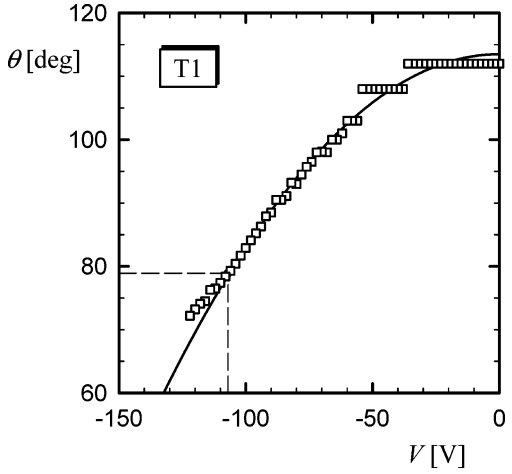

Figure 3. Electrowetting curve (dc voltage), 0.1 M KCl on a 2.0 μm thick Teflon AF (T1). Data are from ref 14. The solid line is the best fit of eq 8 with $\theta_0 = 114°$ and $\beta = 0.42$. Saturation occurs at $\tilde{\theta} = 79°$ and $\tilde{V} = -107$ V. The values calculated through eqs 7 are 78° and −98 V, respectively.

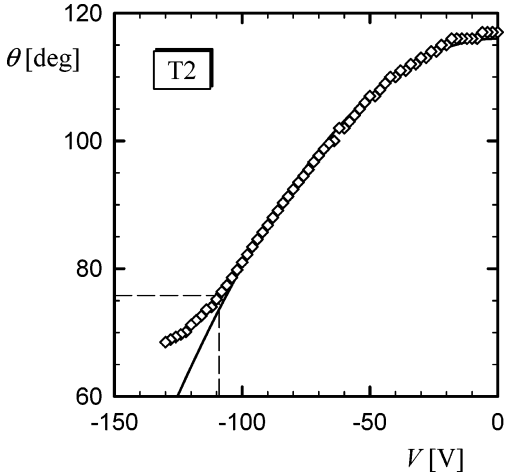

Figure 4. Electrowetting curve (dc voltage), 0.1 M KCl on a 1.8 μm thick Teflon AF (T2). Data are from ref 14. The solid line is the best fit of eq 8 with $\theta_0 = 116°$ and $\beta = 0.44$. Saturation occurs at $\tilde{\theta} = 76°$ and $\tilde{V} = -109$ V. The values calculated through eqs 7 are 80° and −93 V, respectively.

approximation.[47] The working equations of our saturation model are finally written as

$$\tilde{\theta} = \arccos\frac{\gamma_C}{\gamma}$$

$$\tilde{V} = \left[\frac{2(\gamma_C - \gamma\cos\theta_0)}{C}\right]^{1/2} \tag{7}$$

The capacitance per unit area, C, is obtained from the geometry and the dielectric constant, ϵ, of the polymer layer ($C = \epsilon\epsilon_0/d$ for a flat layer of thickness d and $C = \epsilon\epsilon_0/R_2 \ln(R_2/R_1)$ for a cylindrical layer with inner radius R_1 and outer radius R_2; ϵ_0 is the permittivity of vacuum).

By combination of eqs 2 and 5, we obtain the Young−Lippmann relation

$$\cos\theta(V) = \cos\theta_0 + \frac{C}{2\gamma}V^2 \tag{8}$$

This expression is currently adopted as the basis of almost all discussions of the electrowetting effect.

Comparison with Experiments

Three examples of the prediction based on our saturation model, compared with the experimental data, are shown in Figures 3−5. As we have described previously,[14] electrowetting with dc voltage was carried out with 0.1 M KCl water droplets (the droplet was always grounded) on a series of fluoropolymer coatings, members of the Teflon AF family (DuPont). The three random copolymers of tetrafluoroethylene (TFE) and 4,5-difluoro-2,2-bis(trifluoromethyl)-1,3-dioxole (PDD) have different ratios between the two monomers and slightly different surface properties.[14] Since deviations occur when positive voltages are used, we discuss here only the negative branch of the electrowetting curves (an extensive discussion of the full curves has been given elsewhere[14]).

In all three cases, the critical point where data deviate from the Young−Lippmann equation (the solid line) is predicted very convincingly by our model. We have found that when fitting eq 8 a better fit is obtained if the numerical coefficient of the quadratic term is taken as a free parameter, β. Encouragingly, the values of β are generally equal to or near $^1/_2$ but can sometimes vary a little from this. In passing, we note that this is a clear validation of the essential theory (eq 8). In all cases, we calculated the critical contact angle, $\tilde{\theta}$, via eq 3 and then determined the threshold voltage, $\tilde{V}$, from the fitted parabola. It should also be emphasized that in Figures 3−5 the electrowetting curves do not reach a plateau value at $\tilde{V}$ but deviate from the Young−Lippmann equation and then asymptotically level off.

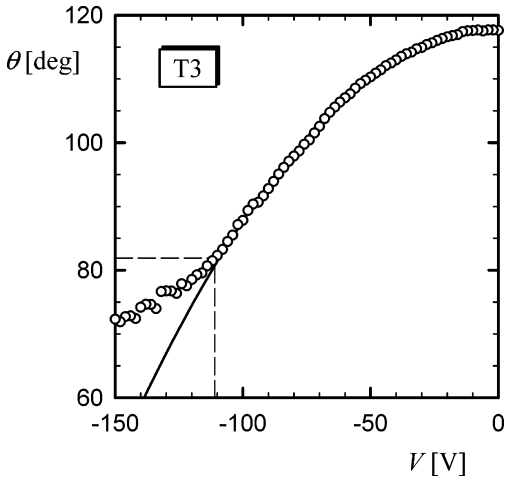

Figure 5. Electrowetting curve (dc voltage), 0.1 M KCl on a 2.4 μm thick Teflon AF1600 (T3). Data are from ref 14. The solid line is the best fit of eq 8 with $\theta_0 = 118°$ and $\beta = 0.54$. Saturation occurs at $\tilde{\theta} = 82°$ and $\tilde{V} = -111$ V. The values calculated through eqs 7 are 80° and −114 V, respectively.

The same type of analysis was applied to published electrowetting curves. As an example, we present in Figure 6 the data of Blake et al.[9] for 60% aqueous glycerol (with 0.4% NaCl) on a 100 μm thick poly(ethylene terephthalate) (PET) tape. The variation of the static contact angle with the applied dc voltage is rather nicely described by the Young−Lipmann equation (the solid line).

The prediction of our eq 3 is shown with a dashed line. The order of magnitude of $\tilde{\theta}$ (and of $\tilde{V}$ correspondingly) is predicted correctly, but the value is overestimated.

Another example (taken from ref 10) is shown in Figure 7. The system is a 75% glycerol/water mixture (with 4 g/L NaCl) on a 100 μm thick poly(tetrafluoroethylene) (PTFE) film. The

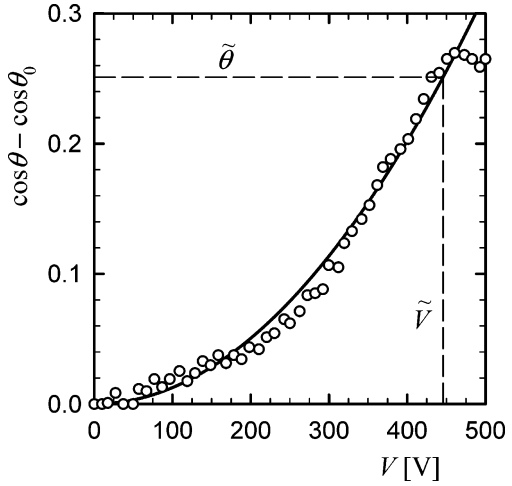

Figure 6. Electrowetting curve (dc voltage), 60% aqueous glycerol with 0.4% NaCl on a 100 μm thick PET tape. Data are from Blake et al.[9] The solid line is the best fit of eq 8 with $\theta_0 = 66°$ and $\beta = 0.29$. Saturation occurs at $\tilde{\theta} = 48°$ and $\tilde{V} = 450$ V. The values calculated through eqs 7 are 49° and 446 V, respectively.

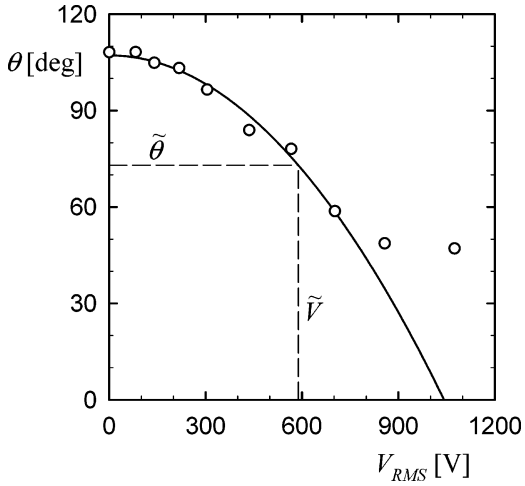

Figure 7. Electrowetting curve (ac voltage), 75% aqueous glycerol with 4 g/L NaCl on a 100 μm thick PTFE film. Data from Decamps and De Coninck.[10] The solid line is the best fit of eq 8 with $\theta_0 = 107°$ and $\beta = 0.58$. Saturation occurs at $\tilde{\theta} = 54°$ and $\tilde{V}_{\mathrm{RMS}} = 780$ V. The values calculated through eqs 7 are 73° and 590 V, respectively.

data follow the trend predicted by eq 8 rather strictly. The saturation angle and voltage predicted by our model (dashed lines in Figure 7) are in broad agreement with the last point belonging to the parabola. Yet again, $\tilde{\theta}$ is higher than the lowest contact angle experimentally observed. Note that the voltage increment used by these authors is rather large (~140 V).

On the whole, the behavior illustrated in Figure 7 is not significantly different from the previous examples even though ac voltage was used in this case (as a consequence the root-mean-square (rms) voltage is used on the abscissa).

In fact, both examples are rather typical of the experimental electrowetting results published in the last years. We have analyzed most of the available data in a similar manner, and a summary outcome is presented in Table 1 (full details have been given in ref 48).

The agreement between the saturation angle predicted by our model, $\tilde{\theta}$, and the various experimental values, θ_{sat}, is often acceptable, but there are also cases where the discrepancy is large. In these latter cases, there appears to be no obvious correlation between compliance with the model and film thickness, critical surface tension, or type of voltage applied.

TABLE 1: Comparison of Predicted and Observed Values of the Contact Angle at Saturation and Beyond[g]

insulator	d (μm)	γ_C (mN/m)	g (mN/m)	voltage type	$\tilde{\theta}_{\mathrm{exp}}$ (deg)	$\tilde{\theta}_{\mathrm{min}}$ (deg)	$\tilde{\theta}_{\mathrm{est}}$ (deg)
Parylene/AF1600[a]	6	12.7	72.8	dc (+)	69	61	80
Parylene/AF1600[a]	10	12.7	72.8	dc (+)	68	60	80
polyimide/AF1600[a]	18	12.7	72.8	dc (+)	68	63	80
polyimide/AF1600[a]	35	12.7	72.8	dc (+)	67	64	80
AF1600[b]	5.8	12.7	72.8	dc (−)	52	50	80
AF1600[b]	0.5	12.7	72.8	dc (+)	95	88	80
PET[c]	100	39.5	64	dc (+)	48	48	52
PET[c]	100	39.5	64	ac	50	43	52
PTFE[d]	100	19	64	ac	54	47	73
PET[e]	12	39.5	72	ac	45	40	57
PTFE[e]	70	18.5	72	ac	54	39	75
PTFE[f]	50	18.5	72	ac	30	27	75

[a] Data from ref 5. [b] Data from ref 6. [c] Data from ref 9. [d] Data from ref 10. [e] Data from ref 3. [f] Data from ref 11. [g] The variables are represented as follows: thickness of the insulating layer, d; Zisman's critical surface tension of the insulating layer, γ_C; liquid surface tension, γ; experimental contact angle at saturation, $\tilde{\theta}_{\mathrm{exp}}$; minimum contact angle beyond saturation, $\tilde{\theta}_{\mathrm{min}}$; saturation contact angle estimated by eq 3, $\tilde{\theta}_{\mathrm{est}}$.

Discussion

The agreement between our model prediction and the published results (analyzed in the previous section) is relatively good. In 7 out of the 12 cases, the difference is within 13°, a very decent performance for such a simple first-approximation model. It must also be stressed that several sources of errors may well obscure the reinterpretation of published results. (i) Minor alterations in the surface preparation protocol or sample handling may cause significant changes in the observed behavior (e.g., all the efforts required to obtain coatings of consistent quality[48] or the dependence of the dielectric strength of such films upon the method of preparation[6]). (ii) It is conceivable that contaminated systems have been used (it has been known that treating a Teflon AF coating with silicone oil often improves electrowetting results;[12] while such an approach is commendable in developing a reliably operating device, it is highly undesirable from a physicochemical point of view). (iii) With few notable exceptions,[49,50] most electrowetting curves were obtained with a rather large voltage increment (20−100 V), and this may have introduced some time-dependent effects (due to undetected slow kinetic changes). Finally, we recall that our model describes rather well another set of results obtained in this laboratory, electrowetting of water on Parylene layers (4, 15, and 30 μm thick) coated with 100 nm of Teflon AF1600.[13]

In our treatment, we have ignored the spreading pressure, i.e., the possible difference between γ_S (relevant for a solid surface exposed to vacuum) and γ_{SV} (characteristic of a solid surface exposed to saturated vapors of the wetting liquid). The topic has been long debated, and the general perception is that for most polymer surfaces (i.e., low-energy surfaces) its influence can be safely neglected.[51,52] The spreading pressure is a decreasing function of the contact angle, and since in electrowetting relatively hydrophobic surfaces are of highest interest, neglecting its influence should not introduce any significant error.

Equation 3 in fact delineates the domain of validity of the Young−Lippmann equation. The thermodynamic limit is $\gamma_{SL} = 0$, and consequently the solid/liquid interface should become unstable. It is common knowledge that if two immiscible liquids are brought together in the presence of specific surfactants (e.g., primary and a cosurfactant), then the interfacial tension can be temporarily altered to zero or even negative values,[53,54] thus providing the driving force for the formation of microemulsions.

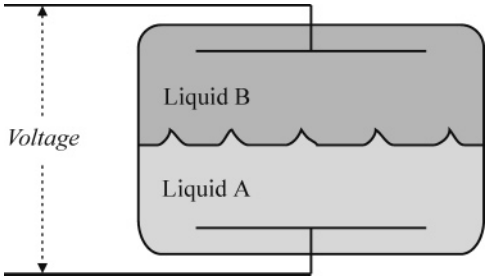

Figure 8. Horizontal fluid interface in a vertical electric field. Fluid B is a perfect insulator while fluid A is perfectly conducting. This arrangement is analogous to the configuration depicted in Figure 1, except that the insulator there is solid (amorphous Teflon AF) and there are no end effects.

In most cases where the liquids are immiscible, the liquid/liquid interfacial tension is positive, and the interface is stable. If liquid A is conductive (e.g., an aqueous electrolyte solution) and liquid B is an insulator (e.g., organic liquid), then dc voltage can be applied across the liquid/liquid interface without significant current flowing through the circuit (Figure 8).

There is a critical voltage above which the interface becomes unstable, initial undulations are followed by the appearance of sharp, drop-emitting peaks of the conducting fluid, which eventually develop into liquid columns.[55−58] The behavior has been observed at various liquid/liquid and liquid/vapor interfaces. According to the theory,[56,57] the critical wavenumber, $\tilde{k}$, is

$$\tilde{k} = \left[\frac{(\rho_B - \rho_A)g}{\gamma_{AB}}\right]^{1/2} \tag{9}$$

where ρ_A and ρ_B are the densities of the two liquids, γ_{AB} is the interfacial tension, and g is the acceleration due to gravity. The critical voltage (for the case where liquid A is a perfect insulator and liquid B is perfectly conductive) is[56,57]

$$\tilde{V} = \left(\frac{2\tilde{k}\gamma}{\epsilon_A\epsilon_0}\right)^{1/2} h \tag{10}$$

where h is the vertical displacement of the interface. If we assume that $h \approx 1/\tilde{k}$, i.e., the perturbation being of the order of the capillary constant (the characteristic length scale at a flat liquid/liquid interface), then eq 10 becomes essentially identical to eq 6. Therefore the nature of the instability (hence the limiting voltage) is one and the same in both cases. The major difference is that the amorphous Teflon AF coatings are solid, i.e., too viscous for the instability to become immediately prominent. The solid surface lacks the inherent mobility of a fluid phase, and therefore the instability will manifest itself over longer time scales or under extreme external influences. Some topographic changes of the insulator (Teflon AF1600) surface after electrowetting at $V_{RMS} > \tilde{V}$ for about 20 s have been reported.[48] The damage is mainly located around the edge of the droplet as found in earlier experiments,[3,11] the reason for that being that the electric field in the immediate vicinity of the droplet edge is maximal.[11,59]

We have used, in eq 7, the critical surface tension instead of the surface tension of the solid, thus ignoring the prescient warning of Zisman that the two are not necessarily equal. Currently, most of the electrowetting experiments are carried out on various types of fluoropolymers (e.g., FEP, Teflon, FC721) that are apolar, i.e., they interact with water through van der Waals interactions only.[45,51] In this case, both the van Oss−Good−Chaudhury theory[45,51,52] or the alternative equation of state approach[34] yields the same result;[47] $\gamma_C = \gamma_S$, thus supporting our assumption.

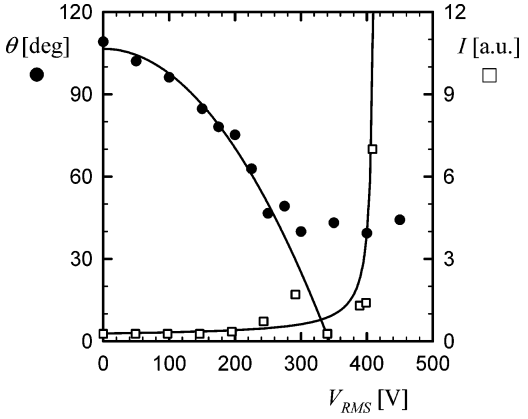

Figure 9. Contact angle, θ, (●) and luminescence intensity, I, (□) as a function of the ac potential, V_{RMS}, applied during electrowetting of 0.1 M KCl on a 9 μm thick layer of Parylene N coated with 0.1 μm Teflon AF1600.

Our model predicts the point of deviation from the parabolic Young−Lippmann eq 8 rather than the lowest contact angle accessible through electrowetting. This is quite obvious in Figures 3−5. From the analysis of our model, it appears that any portion of the electrowetting curve situated at $|V| > |\tilde{V}|$ cannot be at equilibrium.

Two rather dissimilar explanations of the nature of contact angle saturation have been put forward. Vallet et al.[11] have observed simultaneously luminescence around the edge of a droplet (0.01 M aqueous Na_2SO_4 electrowetted with ac voltage on PTFE films) and notable current spikes occurring at a voltage where the contact angle appeared to saturate (the point of deviation from the parabolic curve rather than the plateau value at high voltages was used). The coincidence between the voltage where deviation occurred, i.e., $\tilde{V}$, and the voltage at which luminescence was detected proved to be good for PTFE films of various thickness (12−227 μm) and reportedly for other insulating materials. Berge and co-workers concluded that air ionization is the limiting phenomenon for electrowetting.[11]

We monitored the intensity of luminescence during electrowetting of a 0.1 M KCl water droplet on a layer of Parylene N (9 μm) coated with Teflon AF1600 (0.1 μm) and obtained a somewhat different result (Figure 9). Experimental details are given elsewhere.[48]

Continuous luminescence, hence air ionization, does not occur below approximately 400 V (□ in Figure 10), which is well above the saturation threshold $\tilde{V} \approx 240$ V. Furthermore, no such observation could be made for dc potentials (as high as 600 V) where saturation occurs in a similar manner (Figures 3−5). A good test for the gas ionization hypothesis is to carry electrowetting under the same conditions but in a gas with a different dielectric strength. Vallet et al.[11] did use C_2F_6 (hexafluoroethane) and SF_6 (sulfur hexafluoride) but obtained the same $\tilde{V}$. It is also well-documented that saturation occurs in polymer/water/decane systems and yet no breakdown has been detected.[7] Thus, ionization of the gas in the vicinity of the contact line appears to be a concurring rather than limiting event with respect to electrowetting. Finally, Vallet et al.[11] stress that the saturation angle in their experiments (20−30°) was independent of the film thickness. They argued that most important is the electric field near the droplet border and estimated its maximum value as $E_{max} \cong V/(Rd)^{1/2}$, R being the radius of curvature of the liquid edge. If R remains constant, then V^2/d should also stay constant, and this would imply a constant (saturation) angle through eq

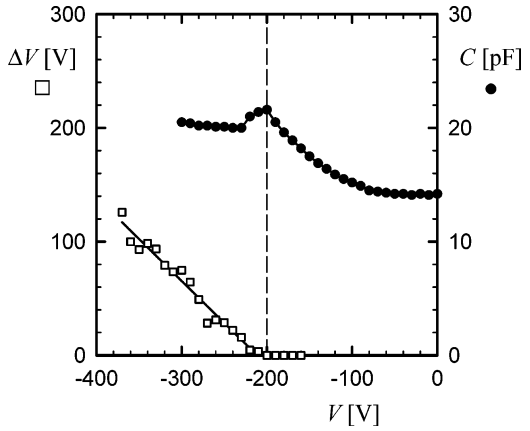

Figure 10. Capacitance, C, (●) and surface potential, ΔV, (□) as a function of the dc potential, V, applied during the electrowetting of 0.1 M KCl on a 9 μm thick layer of Parylene N coated with 0.1 μm Teflon AF1600.

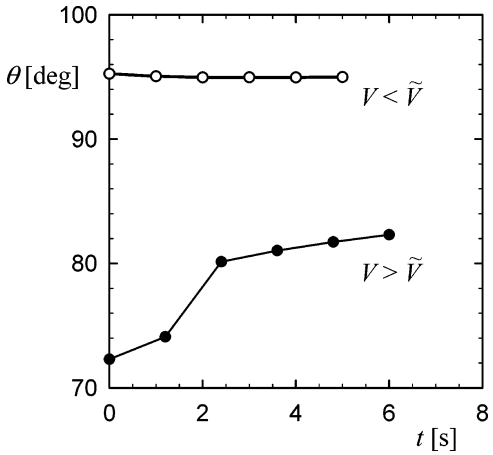

Figure 11. Time dependence of the contact angle, θ, at fixed voltage, V, when electrowetting 0.1 M KCl on a 1.0 μm thick layer of Teflon AF1600: ○, 50 V; ●, 90 V ($\tilde{V} \approx 70$ V).

8. We remark that our model yields the same conclusion but from a very different point of view (the thickness of the insulator, d, does not enter eq 3). Recently Buehrle et al.[38] presented a description of the droplet edge during electrowetting in which the contact angle at the contact line is determined by Young eq 1 and not at all affected by the electrostatic field. In their model, the inclination of the liquid surface away from the contact angle follows the Young−Lippmann eq 8.

Verheijen and Prins[12] offered a very different explanation for electrowetting saturation. They assumed that a certain portion of the charge, which in the Lippmann model is located at the ideally polarizable interface between the solid insulator and the conductive liquid, is in fact injected into the insulating polymer film. Therefore, at any voltage beyond $\tilde{V}$, the actual charge at the interface is less than the amount predicted by Lippmann equation and consequently the efficiency of electrowetting is reduced, i.e., the contact angle decrease is smaller than the value anticipated from eq 8. The Young−Lippmann equation (for a flat insulating layer) was modified to[12]

$$\cos\theta(V) = \cos\theta_0 + \frac{\epsilon\epsilon_0}{2\gamma d}(V - V_T)^2 \qquad (11)$$

The V_T correction is formally related to the area charge density, σ_T, of a layer of charge effectively located at a depth z under the insulator/liquid surface

$$V_T = \frac{\sigma_T}{\epsilon\epsilon_0}(d - z) \qquad (12)$$

This hypothesis is quite popular probably due to its simplicity and the fact that charge injection (or charge trapping) is a well-known effect. Charge transfer occurs across the solid/liquid interface between an insulator and a nonwetting conductive liquid[60] and has been used to produce electrets.[61,62] In the Verheijen−Prins scenario, however, trapped charge is already present ahead of the liquid droplet (Figure 2b in ref 12). This is rather unexpected for a droplet electrowetting a fresh surface, and these authors invoked "excitations of the droplet, e.g., thermal, mechanical, or voltage-induced vibrations" to provide a mechanism for charge creation. It appears to us that such "excitations" are not dominant, if present at all, as long as the Young−Lippmann equation is obeyed. Therefore, for charge injection to play the limiting phenomenon in eletrowetting, it must come into play at exactly $\tilde{V}$ and be more and more efficient at any $V > \tilde{V}$. Whether this is entirely true remains to be proven.

There is a notable similarity between the saturation part of an electrowetting curve and the charge-transfer curves for charging of FEP (a copolymer of tetrafluoroethylene and hexafluoropropylene) foils with various charging liquids.[62] The outcome of our own experiment with a 0.1 M KCl electrowetted on a layer of Parylene N (9 μm) coated with Teflon AF1600 (0.1 μm) is shown in Figure 10. Electrowetting saturation occurs at about 200 V negative potential (dashed line in Figure 10) as determined by monitoring the capacitance (● in Figure 10).

In the same system, numerous electrowetting switches (from zero to a fixed dc potential) have been performed on a single droplet. The droplet was then removed, and the charging of the substrate was probed with an electrostatic voltmeter (see ref 48 for details). The readings (□ in Figure 10) depart from zero below a threshold voltage of about −210 V. Thus, the onset of saturation coincides with a significant charge being left behind the electrowetting droplet.

It is conceivable that $\gamma_{SL} = 0$, the critical condition in our equilibrium model, is a necessary (if not sufficient) condition for charge injection because if $\gamma_{SL} > 0$ it will act as a barrier to charge carrier transport across the interface. Therefore, our model does not reject the charge injection mechanism but rather provides an alternative, more formal route to assess contact angle saturation.

As already noted, according to our analysis, the portion of the electrowetting curve located beyond $\tilde{V}$ is essentially non-equilibrium. Indeed, as can be seen in Figure 11, the contact angle at a fixed voltage remains constant as long as the voltage does not exceed the critical value; however, it drifts up when $V > \tilde{V}$.

In other words, contact angles on one and the same electrowetting curve have different meanings depending on the voltage relative to $\tilde{V}$. Minimum contact angles, which understandably are of great technical interest, are essentially time-dependent. The behavior illustrated in Figure 11 suggests that if electrowetting is carried out fast enough, then lower contact angles may be reached. A further confirmation of the importance of kinetic effects is shown in Figure 12.

The two electrowetting curves coincide in the Young−Lippmann (equilibrium) region (except for a small shift in the contact angle at zero volts, which can be attributed to slight variations in the sample quality). At higher voltages, however, the difference is very significant. With the smaller increment, we found $\tilde{V} \approx -130$ V and $\tilde{\theta} = 79°$, in good agreement with eqs 7. With the larger increment, the threshold voltage is −150

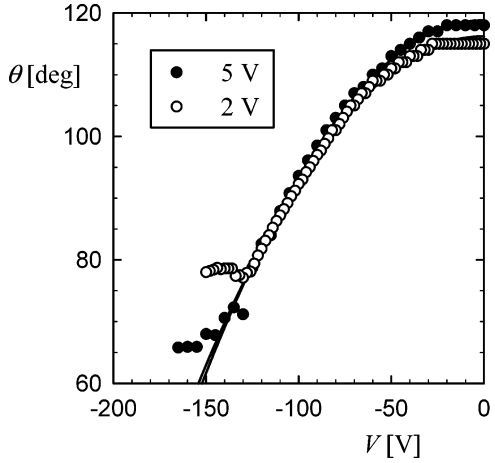

Figure 12. Electrowetting curves for 0.1 M KCl on a 2.4 μm thick layer of Teflon AF1600 obtained with different voltage increments: ○, 2 V; ●, 5 V.

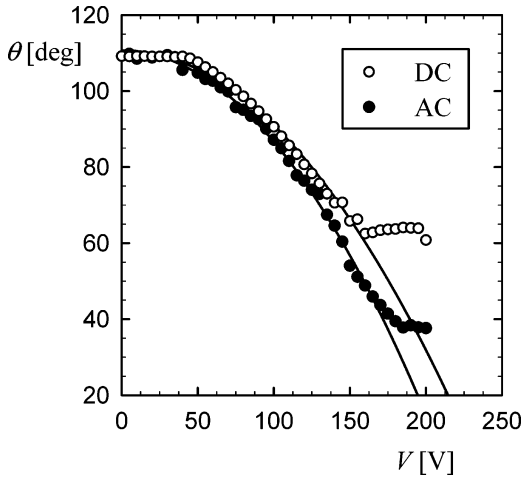

Figure 13. Electrowetting curves for 0.1 M KCl on a layer of Teflon AF (T1) obtained with dc voltage (○) and ac voltage (●) (in this case V_{RMS} is used on the abscissa).

V, and the saturation angle drops to about 65°. For the same system, Seyrat and Hayes[6] observed saturation angles as low as 50° when using a 30 V step. The size of the voltage increment thus appears to be a significant factor that has been overlooked in the past.

Finally, electrowetting with dc and ac voltages are similar but not equivalent (Figure 13).

Yet again, the correspondence between the two curves is rather good in the parabolic region, but saturation is postponed when ac voltage is employed. Consequently, lower saturation angles are achievable, which might be a significant advantage in some applications. The difference is most easily explained with the charge injection hypothesis; at ac voltage, the charge carriers lag behind the electric field, and this effectively reduces the rate of transport across the interface. Indeed the response time for dc voltages is about 15 ms[4] while for ac potentials contact angles reach plateau values after 100 ms to several minutes or more.[10] This nonequilibrium electrowetting behavior at ac potentials is reminiscent of the transient negative interfacial tensions observed during microemulsion formation, reflecting interfacial transport processes.[53,54]

Conclusion

Our attempt to quantify the saturation limit appears to be moderately successful. We have estimated the thermodynamic limit beyond which the contact angle will not obey the Young−Lippmann equation. The predictive power of our model is sound, if limited, and is firmly based on material properties, as in the original Lippmann equation. It applies rather well to systems where dc voltages are applied. At ac voltages, lower contact angle values can be reached via electrowetting but arguably involve nonequilibrium effects, which do require further investigation. Our approach does not necessarily negate other hypotheses but rather offers an alternative (and more formal) route to assess contact angle saturation.

Acknowledgment. Financial support for this project from the Australian Research Council Special Research Centre Scheme is gratefully acknowledged as well as from Philips Research, Eindhoven, The Netherlands. The support of R. Hayes and J. Feenstra (Philips) and C. Quilliet (Grenoble) is warmly acknowledged.

References and Notes

(1) Quilliet, C.; Berge, B. *Curr. Opin. Colloid Interface Sci.* **2001**, *6*, 34.
(2) Berge, B. *C. R. Acad. Sci. Ser., IIc: Chim.* **1993**, *317*, 157.
(3) Vallet, M.; Berge, B.; Vovelle, L. *Polymer* **1996**, *37*, 2465.
(4) Verheijen, H. J. J.; Prins, M. W. J. *Rev. Sci. Instrum.* **1999**, *70*, 3668.
(5) Welters, W. J. J.; Fokkink, L. G. J. *Langmuir* **1998**, *14*, 1535.
(6) Seyrat, E.; Hayes, R. A. *J. Appl. Phys.* **2001**, *90*, 1383.
(7) Janocha, B.; Bauser, H.; Oehr, C.; Brunner, H.; Goepel, W. *Langmuir* **2000**, *16*, 3349.
(8) Schneemilch, M.; Welters, W. J. J.; Hayes, R. A.; Ralston, J. *Langmuir* **2000**, *16*, 2924.
(9) Blake, T. D.; Clarke, A.; Stattersfield, E. H. *Langmuir* **2000**, *16*, 2928.
(10) Decamps, C.; De Coninck, J. *Langmuir* **2000**, *16*, 10150.
(11) Vallet, M.; Vallade, M.; Berge, B. *Eur. Phys. J. B* **1999**, *11*, 583.
(12) Verheijen, H. J. J.; Prins, M. W. J. *Langmuir* **1999**, *15*, 6616.
(13) Peykov, V.; Quinn, A.; Ralston, J. *Colloid Polym. Sci.* **2000**, *278*, 789.
(14) Quinn, A.; Sedev, R.; Ralston, J. *J. Phys. Chem. B* **2003**, *107*, 1163.
(15) Jones, T. B. *Langmuir* **2002**, *18*, 4437.
(16) Colgate, E.; Matsumoto, H. *J. Vac. Sci. Technol.,, A* **1990**, *8*, 3625.
(17) Washizu, M. *IEEE Trans. Ind. Appl.* **1998**, *34*, 732.
(18) Pollack, M. G.; Fair, R. B.; Shenderov, A. D. *Appl. Phys. Lett.* **2000**, *77*, 1725.
(19) Cho, S. K.; Moon, H. J.; Kim, C. J. *J. Microelectromech. Syst.* **2003**, *12*, 70.
(20) Prins, M. W. J.; Welters, W. J. J.; Weekamp, J. W. *Science* **2001**, *291*, 277.
(21) Berge, B.; Peseux, J. *Eur. Phys. J. E* **2000**, *3*, 159.
(22) Yang, S.; Krupenkin, T. N.; Mach, P.; Chandross, E. A. *Adv. Mater.* **2003**, *15*, 940.
(23) Hayes, R. A.; Feenstra, B. J. *Nature* **2003**, *425*, 383.
(24) Shapiro, B.; Moon, H.; Garrell, R. L.; Kim, C. J. *J. Appl. Phys.* **2003**, *93*, 5794.
(25) Adamson, A. W.; Gast, A. P. *Physical Chemistry of Surfaces*, 6th ed.; Wiley: New York, 1997.
(26) de Gennes, P. G. *Rev. Mod. Phys.* **1985**, *57*, 827.
(27) Everett, D. H. *Pure Appl. Chem.* **1980**, *52*, 1279.
(28) Hurd, R. M.; Schmid, G. M.; Snavely, E. S., Jr. *Science* **1962**, *135*, 791.
(29) Johnson, C. *Nature* **1963**, *197*, 1092.
(30) Sato, M.; Kudo, N.; Saito, M. *IEEE Trans. Ind. Appl.* **1998**, *34*, 294.
(31) Habib, M. A.; Bockris, J. O. M. Specific Adsorption of Ions. In *Comprehensive Treatise of Electrochemistry*; Bockris, J. O. M., Conway, B. E., Yeager, E., Eds.; Plenum Press: New York, 1980; Vol. 1; p 135.
(32) Damaskin, B. B.; Petrii, O. A. *Introduction to Electrochemical Kinetics*, 2nd ed.; Vyshaya Shkola: Moscow, 1983 (in Russian).
(33) White, L. R. *J. Chem. Soc., Faraday Trans. 1* **1977**, *73*, 390.
(34) Neumann, A. W.; Spelt, J. K. *Applied Surface Thermodynamics*; Surfactant Science Series; Marcel Dekker: New York, 1996; Vol. 63.
(35) Rowlinson, J. S.; Widom, B. *Molecular Theory of Capillarity*; Clarendon Press: Oxford, 1984.
(36) Rusanov, A. I. *Solid State Ionics* **1995**, *75*, 275.
(37) Eustathopoulos, N.; Nicholas, M. G.; Drevet, B. *Wettability at High Temperatures*; Pergamon: Amsterdam, 1999.

(38) Buehrle, J.; Herminghaus, S.; Mugele, F. *Phys. Rev. Lett.* **2003**, *91*, 086101/1.
(39) Bockris, J. O. M.; Reddy, A. K. N. In *Modern Electrochemistry*; Plenum Press: New York, 1970; Vol. 2, Ch. 7.
(40) Sondag-Huethorst, J. A. M.; Fokkink, L. G. J. *J. Electroanal. Chem.* **1994**, *367*, 49.
(41) Sondag-Huethorst, J. A. M.; Fokkink, L. G. J. *Langmuir* **1994**, *10*, 4380.
(42) Sparnaay, M. J. *Surface Sci.* **1964**, *1*, 213.
(43) Fokkink, L. G. J.; Ralston, J. *Colloids Surf.* **1989**, *36*, 69.
(44) Landau, L. D.; Lifshitz, E. M. *Electrodynamics of Continuous Media*; Pergamon Press: Oxford, 1960; Vol. 8.
(45) van Oss, C. J. *Interfacial Forces in Aqueous Media*; Marcel Dekker: New York, 1994.
(46) Zisman, W. A. *Adv. Chem. Ser.* **1964**, *43*, 1.
(47) Sedev, R.; Fabretto, M.; Ralston, J. *J. Adhes.* **2004**, *80*, 497.
(48) Quinn, A. Electrowetting Fundamentals: An Investigation Into Deviations From Ideal Behaviour. Ph.D. Thesis, University of South Australia, 2003.
(49) Moon, H.; Cho, S. K.; Garrell, R. L.; Kim, C.-J. *J. Appl. Phys.* **2002**, *92*, 4080.
(50) Saeki, F.; Baum, J.; Moon, H.; Yoon, J.-Y.; Kim, C.-J.; Garrell, R. L. *Polym. Mater. Sci. Eng.* **2001**, *85*, 12.
(51) Good, R. J. *J. Adhes. Sci. Technol.* **1992**, *6*, 1269.
(52) Good, R. J.; van Oss, C. J. In *Modern Approaches to Wettability*; Schrader, M. E., Loeb, G. I., Eds.; Plenum Press: New York, 1992; p 1.
(53) Gerbacia, W.; Rosano, H. L. *J. Colloid Interface Sci.* **1973**, *44*, 242.
(54) Hunter, R. J. *Foundations of Colloid Science*; Clarendon Press: Oxford, 1989; Vol. 2.
(55) Terasawa, H.; Mori, Y. H.; Komotori, K. *Chem. Eng. Sci.* **1983**, *38*, 567.
(56) Taylor, G. I.; McEwan, A. D. *J. Fluid Mech.* **1965**, *22*, 1.
(57) Dong, J. H.; de Almeida, V. F.; Tsouris, C. *J. Colloid Interface Sci.* **2001**, *242*, 327.
(58) Gonzalez, H.; Neron de Surgy, G.; Chabrerie, J. P. *Phys. Rev. B* **1994**, *50*, 2520.
(59) Quinn, A.; Attard, P. *Rev. Sci. Instrum.* **2003**, *74*, 2517.
(60) Engelbrecht, R. S. *J. Appl. Phys.* **1974**, *45*, 3421.
(61) Chudleigh, P. W. *Appl. Phys. Lett.* **1972**, *21*, 547.
(62) Chudleigh, P. W. *J. Appl. Phys.* **1976**, *47*, 4475.